Heliyon 9 (2023) e21200

Contents lists available at ScienceDirect

Heliyon

journal homepage: www.cell.com/heliyon

Facet-occiput slope angle: A novel predictor of cage placement feasibility during surgery in basilar invagination patients

Mirwais Alizada [a], Yuqiang Wang [a], Yao Zhao [a], Shuhao Zhang [a], Gati Hayatullah [b], Min Zhang [a], Shuxin Li [c], Mujahid Alizada [d], Muhibullah Alizada [e], Kejdi Lalaj [f], Kerong Yang [a], Ismatullah Soufiany [g], Limin Wang [a,*], Yilin Liu [a,**]

[a] *Department of Orthopedics, First Affiliated Hospital of Zhengzhou University, Zhengzhou, Henan, PR China*
[b] *Department of Gynecology, First Affiliated Hospital of Zhengzhou University, Zhengzhou, Henan, PR China*
[c] *Department of Imaging Diagnosis, First Affiliated Hospital of Zhengzhou University, Zhengzhou, Henan, PR China*
[d] *Department of Neurosurgery, The Second Affiliated Hospital of Fujian Medical University, Quanzhou, Fujian, PR China*
[e] *Department of Interventional Radiology, First Affiliated Hospital of Zhengzhou University, Zhengzhou, Henan, PR China*
[f] *Department Maxillofacial Surgery, First Affiliated Hospital of Zhengzhou University, Zhengzhou, Henan, PR China*
[g] *Department of Neurology, Nanjing First Hospital, Nanjing, Jiangsu, PR China*

ARTICLE INFO

Keywords:
Basilar invagination
Atlantoaxial dislocation
Facet-occiput slope angle
3D-printed cage
O–C_2a

ABSTRACT

Background and aim: Direct posterior reduction and manipulation of the $C_{1\text{-}2}$ joints, accompanied by placement of spacers, is the state-of-the-art technique for treating basilar invagination (BI) and atlantoaxial dislocation (AAD). The hindrance of occiput to reaching up to the true atlantoaxial facets (AAF) during the surgery remains challenging for cage placement. The aim of this study was to explore an objective and precise method of measuring the effect of the hindrance of occiput to reaching up to the true AAF and cage placement during surgery.
Method: We collected the clinico-imaging data of 58 patients with BI and AAD (Group A) who underwent surgery in our hospital, and 78 control cohorts (Group B) were retrieved retrospectively. We measured facet-occiput slope angle (FOSA) in midsagittal CT. Patients were positioned prone for surgery based on preoperative flexion O–C_2a, and access to the true AAF was observed intraoperatively. The cut-off value of FOSA for the feasibility of cage placement in BI and AAD patients was appointed when access to the true AAF was impossible due to the hindrance of occiput during surgery.
Results: The cut-off value of FOSA for the feasibility of cage placement was 34^o with an area under the curve AUC of 0.800 (95 % CI: 0.672–0.928, $P < 0.001$) and the Youden index of 0.607. In patients with FOSA >34^{o,} reaching up to the true AAF and 3D-printed cage placement was impossible. FOSA was negative in Group A and positive in Group B, significantly larger in females compared to males in both groups and significantly larger postoperatively in Group A.
Conclusion: FOSA can objectively measure the feasibility of cage placement when the patient is positioned prone per preoperative flexion O–C_2a. A FOSA >34^o is contraindication for cage placement.

* Corresponding author.Department of orthopedics, First Affiliated Hospital of Zhengzhou University, No.1 Jianshe East Road, Zhengzhou, 450052, PR China.
** Corresponding author.Department of orthopedics, First Affiliated Hospital of Zhengzhou University, No.1 Jianshe East Road, Zhengzhou, 450052, PR China.
E-mail addresses: gu2keo@126.com (L. Wang), liu212381@126.com (Y. Liu).

https://doi.org/10.1016/j.heliyon.2023.e21200
Received 13 April 2023; Received in revised form 10 October 2023; Accepted 18 October 2023

1. Introduction

BI combined with AAD is a common congenital deformity of the craniocervical junction (CVJ) without known etiology [1]. Direct posterior reduction and manipulation of the $C_{1\text{-}2}$ joints followed by fusion and fixed with spacers have substituted transoral decompression with posterior fusion as the primary therapeutic strategy for BI and AAD [2–8]. Spacers utilization is essential if the posterior approach alone is used because AAD would reduce without spacers, but the vertical slippage and mobility would persist [9].

In severe cases, it is challenging to access the true AAF intraoperatively. Chandra et al. [10] divided the AAF into three categories based on sagittal inclination (SI), and in type III (SI > 160°), the spacer was placed in pseudo-joints instead of true AAF. Salunke et al. [11] proposed the idea of pseudofacets cage placement when hindrance of the visualization and reaching up to the true facets exists. The inclination orientation of AAF in the sagittal plane, its effect on atlantoaxial dislocation, and access to the true AAF have been well documented in previous studies [2,12,13]. However, we could not find any specific method in the literature that can predict the intraoperative hindrance of the occipital bone to access the true AAF and the feasibility of cage placement in patients having BI and AAD. The primary goal of this study was to propose a new angle, which is FOSA, that can predict the intraoperative access up to the true AAF and feasibility of cage placement.

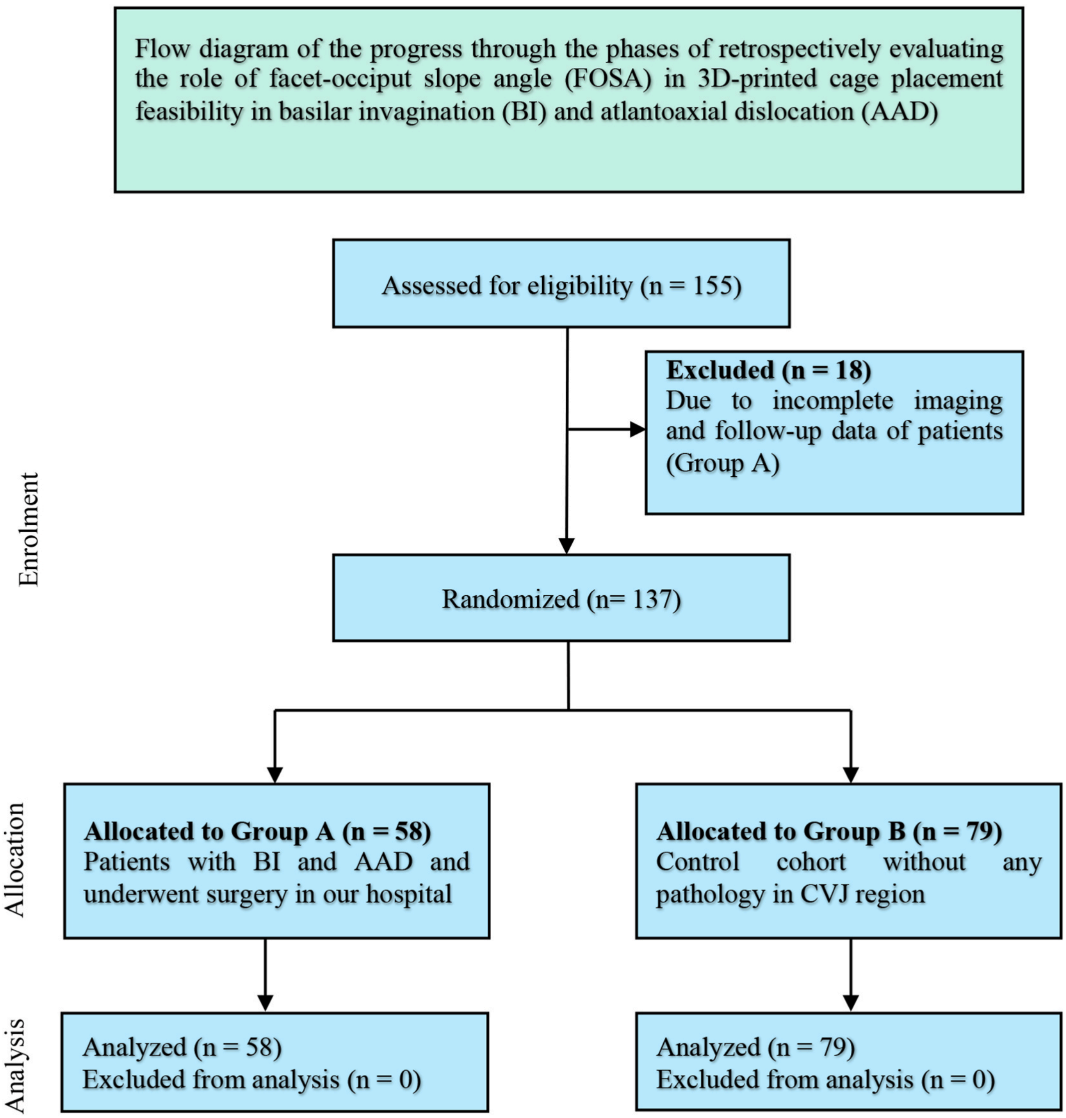

Fig. 1. Flow diagram of the study population.

2. Materials and methods

2.1. Patients selection and study protocols

Initially, clinical and radiological data of 76 patients (Group A) who presented with clinical manifestations of brainstem dysfunction and/or lower cranial neuropathies and with VD > 5 mm and ADI >3 mm on sagittal CT images and underwent surgery in our hospital were analyzed retrospectively between January 1, 2019, and July 30, 2022. The inclusion criteria were: Patients clinically and radiologically diagnosed with BI and AAD, with or without assimilation; had one or more BI and AAD phenotypic features; and had complete imaging and follow-up data. Eighteen cases were excluded due to incomplete imaging and/or follow-up data. Patients with any known genetic syndromes, tumors, the trauma of CVJ, severe osteoporosis, and congenital spinal dysplasia; young patients due to bone immaturity; segmentation abnormalities of CVJ; and incomplete imaging and follow-up data were exclusion criteria (Fig. 1). Finally, 58 patients (19 men and 39 women; mean age, 50.97 ± 13.56 years; range, 18–80 years) with complete imaging data were included in this study with a mean duration of 9 years from symptom onset to the clinic visit.

We recruited 79 consecutive control subjects (Group B) (48 men and 31 women; mean age, 51.72 ± 10.91 years; range, 26–78 years) who had an X-ray and CT of the cervical spine, including CVJ region for suspected spinal trauma, tumor, or stomatology problems. However, there was no evidence of radiographic abnormalities in any of these subjects.

This study was approved by the ethics committee of the First Affiliated Hospital of Zhengzhou University, and informed consent was obtained from all the patients.

Technical Description of the Surgical Technique: All the patients were placed in the prone position with flexed cervical spine based on the preoperative flexion O–C_2a (Fig. 2A). After standard exposure, the occipital squama, upper cervical spinous process, laminae, and the atlantoaxial joint capsules were exposed with meticulous dissection and cranial retraction of the C_2 root for intraarticular fusion. In all patients, lateral mass screws were used [14,15] except in cases in which the atlas posterior arch defect or abnormal course of the vertebral artery where an occipital plate was utilized. Pedicle screws [16] were favored for axis fixation as they provide greater fixation strength, but laminar screws [17] were chosen if the pedicle was too small to accommodate a screw, as determined from the preoperative CT scans.

The AAF was opened and distracted with osteotomes, articular cartilages were removed, and a 3D-printed cage packed with morselized autologous bone was placed. The pre-bent titanium rods (3.5 mm) were placed between the C_1–C_2/occiput-C_2 polyaxial screws tulips and fastened over the C_2 screw head but loosely held in position over the C_1/occiput screw head. The traction load was removed and brought the head to the neutral position with simultaneous down-pressing of the spinous process of the axis to move the odontoid process forward and downward, followed by locking the C_1/occipital screw's nut. Finally, posterior bony cortices were decorticated to prepare a fresh bone bed. A composite bone was grafted for posterior fusion. Intraoperative neuromonitoring was performed. The final construct was confirmed with fluoroscopy (Fig. 2B).

2.2. Radiographic measurement

Odontoid view (open mouth odontoid view), lateral static and dynamic radiographs, CT (1-mm section in neutral position with reconstruction), and MRI (plain and contrast views, 1.5T) of the cervical spine including CVJ region were performed preoperatively and soon after surgery in all patients. Magnetic resonance angiography (MRA) was only performed preoperatively. Roentgenographs and CT scans were obtained on the first follow-up visit (3 months postoperatively) to observe construct position and bone fusion rate between C_1 and C_2 or O–C_2.

An experienced radiologist with over 30 years of experience in neuroimaging and a professor of orthopedics and spine surgery with

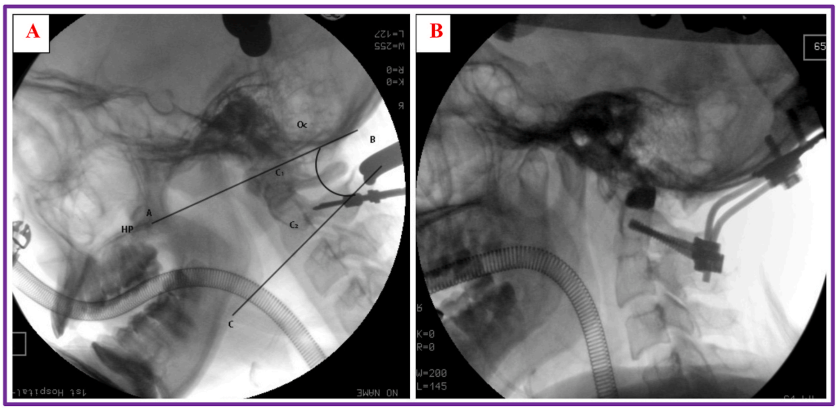

Fig. 2. A: Lateral C-Arm radiograph of the patient to confirm the flexion position in accordance with preoperative flexion O–C_2a (<ABC). The radiograph is taken after the patient is positioned prone and before the opening up of the lateral atlantoaxial joint. Oc: occiput, C_1: atlas vertebra, C_2: axis vertebra, HP: hard palate; **B**: Intraoperative lateral C-Arm radiograph showing position of the cage and final construct.

more than 35 years of experience in this field performed the measurements, and the average was calculated. We measured FOSA, O–C_2 angle (O–C_2a), atlantodental interval (ADI), cervicomedullary angle (CMA), and vertical distance (VD).

FOSA is formed between the line drawn from the lateral atlantoaxial facet to the occiput and another line drawn parallel to the inferior facet of the atlas in the parasagittal CT view (Fig. 3A–D). The angle is drawn in reference to the midpoint of the lateral mass of the axis in the mid-coronal CT view, which is 14 mm on average from the long axis of the odontoid process [18,19]. The long axis of the odontoid process is the line joining the midpoints of the C_2 and C_3 uncinate processes to the tip of the odontoid process [20]. FOSA is positive if the occiput is located above the level of the lateral atlantoaxial facet in the sagittal view and negative when the occiput is located below the AAF level. O–C_2a is subtended between McGregor's line and the inferior endplate of C_2 and measured on lateral X-ray (Fig. 3E and F) [21]. ADI is the shortest distance between the posterior point of the anterior C_1 arch and the dens body junction in

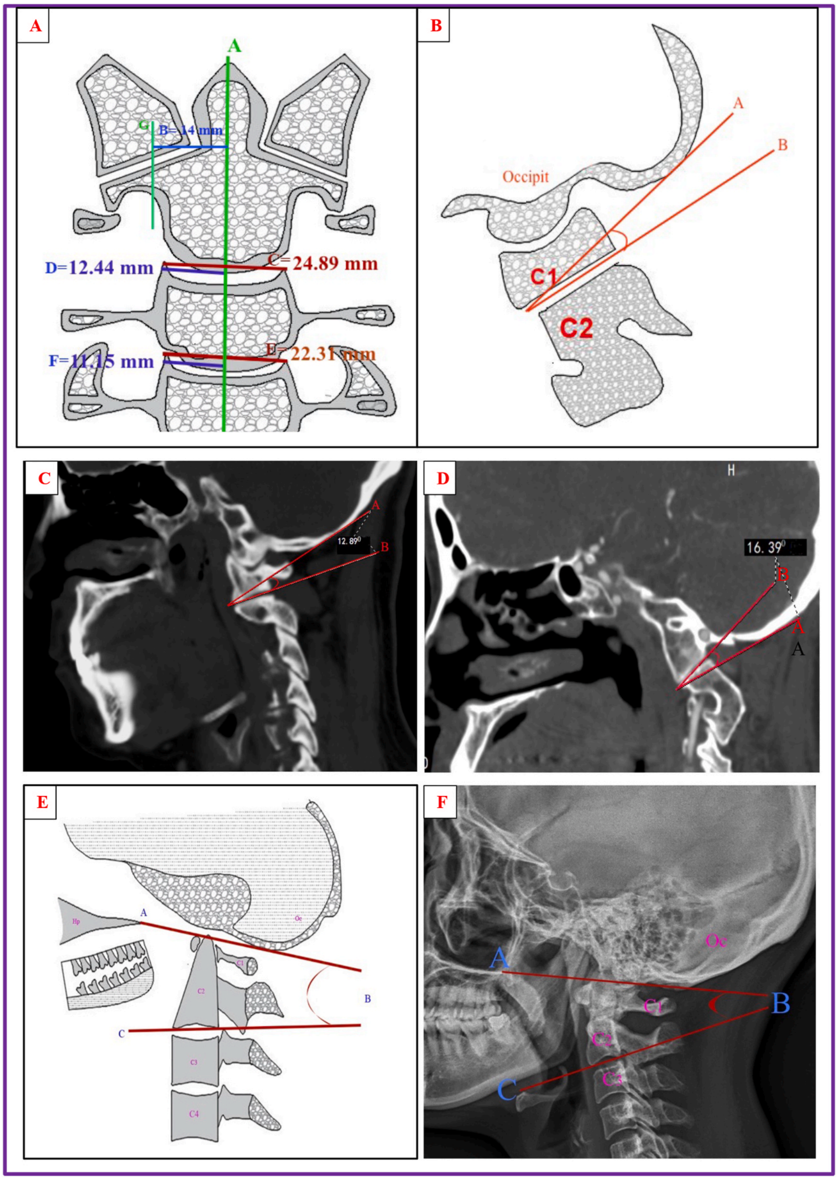

Fig. 3. **A&B**: Schematic representation of FOSA. In reference to the midpoint of the lateral mass of axis on mid-coronal CT view (*green line A)*, which is 14 mm on average from the long axis of the odontoid process [18,19]**A**, on para-sagittal view **B**, *line A(red)* is drawn from the lateral atlantoaxial facet to the occiput, and line *B(red)* is drawn parallel to the inferior facet of atlas; the angle formed by *line A* and *B* on parasagittal view is FOSA. The long axis of the odontoid process is the line joining the midpoints of the C_2 and C_3 uncinate processes to the tip of the odontoid process [20]. In parasagittal view, *line A* is fixed while *line B* changes with the caudorostral position of the occiput relative to the lateral atlantoaxial articulation. If *the occiput* is located above the level of the lateral atlantoaxial facet on sagittal view, FOSA is positive, while FOSA is negative when the *occiput* is located below the joint level; **C**: positive FOSA as *line B* located below *line A*; **D**: Negative FOSA as *line B* located above *line A*. **E**: Sketch of O–C_2 angle formed by McGregor line and base of C_2 vertebra, Hp = Hard palate, Oc: occiput, **F**: O–C_2a in cervical lateral static X-ray < ABC.

the sagittal CT scan [22]. In MRI view, CMA is formed between the line parallel to the anterior side of the medulla oblongata and the line parallel to the ventral side of the upper cervical spinal cord [23].

VD is measured between Chamberlain's line and the odontoid tip in the midsagittal CT view. Negative VD denotes the odontoid tip rostral to Chamberlain's line and positive verse versa.

2.3. Statistical analysis

All values were stated as mean ± standard deviation. We used the chi-square and independent-sample *t*-test to compare the categorical and continuous variables between the groups, Pre- and postoperative imaging parameters were compared using the paired-samples *t*-test. The intraclass correlation coefficient (ICC) was used to investigate the reproducibility of measures between the examiners. The correlation between two continuous values was examined using the Pearson correlation coefficient. The receiver operative curve (ROC) of FOSA was reconstructed, and the area under the curve (AUC) was calculated to identify the accuracy of this parameter in predicting the feasibility of cage placement. FOSA was considered of high accuracy if AUC is > 0.9, while 0.7 to 0.9 indicates moderate accuracy [23]. The optimal cut-off value of FOSA for predicting the feasibility of cage placement was determined by the ROC curve using the Youden index (J) [24,25]. We used a multiple regression analysis to examine the association of FOSA with either OC_2a or CMA, with FOSA as the dependent variable. The independent variables were age, sex, OC_2a, and CMA. The value was taken as statistically significant when a two-tailed $a < 0.05$.

3. Results

3.1. Patient characteristics

In Group A, the interval of symptoms was from 7 months to 19 years (mean ± SD, 9.62 ± 5.83 years). Progressive quadriparesis (89.66 %) was the leading complaint, followed by head and neck pain (67.24 %) and unsteady gait (51.72 %). Among the associated pathologies, vertebral artery anomalies were the foremost accompanied pathology (55.17 %), followed by K–F syndrome (53.45 %) and $O–C_1$ assimilation (51.72 %). The sex difference between the two groups was statistically significant ($P = 0.002$) (Table 1). The number of females was higher than males in the patients' group and vice versa in the control cohort.

3.2. Clinical outcomes

There were no postoperative neurological deterioration or swallowing difficulties. Fifty-three (91.38 %) patients improved clinically, and 4 (6.9 %) had stable symptoms. One patient (1.72 %) in the transoral procedure had postoperative wound and upper respiratory tract infections and died in the intensive care unit (ICU). There was no cerebrospinal fluid (CSF) leakage, cage subsidence, or displacement in any patients. Two patients of the posterior fusion procedure had surgical site infections and healed after antibiotics infusion and dressing.

3.3. Radiological analyses

FOSA was positive in Group B (100 %), while in Group A, it was negative 62.1 % and 75.9 % on the right and left sides, respectively. The $O–C_2a$-NP, $O–C_2a$-Hp, and CMA showed significantly smaller values in Group A than in Group B ($P < 0.05$) (Table 2). Females showed a larger mean value of FOSA in both groups (both sides, $P < 0.0$) (Table 3). In Group A, $O–C_2a$-NP showed a significantly larger mean value in males than in females ($P < 0.05$), but this difference was insignificant in Group B ($P = 0.426$). Compared to the preoperative period, the mean value of negative FOSA significantly decreased on both sides ($P < 0.001$), and the mean value of CMA significantly increased after surgery ($P < 0.001$) (Table 4).

The ROC showed that FOSA had moderate accuracy in predicting cage placement feasibility with an AUC of 0.800 (95 % CI: 0.672–0.928, $P < 0.001$). The optimal cut-off point was 34^o, with 85 % sensitivity and 75.7 % specificity (Fig. 4). The Youden index

Table 1
Demographic data of study population (both groups).

Characteristics	Group-A (58)	Group-B (79)	χ^2/*t*-Value	*P*-value
	N (%)	N (%)		
Sex				
Male	19(32.8 %)	48(60.8 %)	10.494	0.002[a]
Female	39(67.2 %)	31 (39.2 %)		
Age(years) Mean ± SD	50.91 ± 13.69	51.72 ± 10.91	−0.384	0.702[b]
Diabetes	10(16.95 %)	12(15.00 %)	0.097	0.756[a]
Hypertension	8(13.56 %)	10(12.5 %)	0.034	0.854[a]
Active smoker	20(33.90)	37(46.25 %)	2.142	0.143[a]

[a] Chi-square test.
[b] independent sample t-tes.

Table 2
Preoperative parameters compared between patients and control cohort.

Parameters	Group-A	Group-B	*t*-Value	*P*-Value
	Mean ± SD	Mean ± SD		
FOSA –R(°)	−19.25 ± 17.32(+2.69 to −73.01)	20.52 ± 6.05(5.76–33.04)	−0.535	0.594
FOSA -L(°)	−17.42 ± 11.14(+2.74 to −50.60)	18.71 ± 7.14(5.58–39.15)	−0.775	0.44
ADI (mm)	5.48 ± 2.50 (0.63–12)	1.33 ± 0.57(0.30–3.18)	12.413	<0.001
O–C_2a-Np(°)	10.15 ± 5.61(2.29–28.07)	18.89 ± 7.36 (2.14–36.49)	−7.827	<0.001
O–C_2a-HP(°)	8.91 ± 5.22(0.84–25.24)	11.64 ± 6.67 (1.68–26.55)	−2.117	0.037
VD (mm)	−11.41 ± 3.37(-5.05 to −22.15)	2.92 ± 2.03(0.00–7.78)	17.056	<0.001
CMA(°)	131.58 ± 9.30(118.84–150.40)	153.37 ± 19.72(136.35–174.29)	−7.740	<0.001

FOSA-R: facet-occiput slope angle on right side; FOSA-L: facet-occiput slope angle on left side; O–C_2a-Np:O–C_2 angle in neutral position; O–C_2a-HP: O–C_2 angle in hyperflexion position; VD: vertical distance; CMA: cervicomedullary angle.

Table 3
Preoperative parameters compared between males and females in both groups.

Parameters	Group-A				Group-B			
	Male	Female	*t*-Value	*P*-Value	Male	Female	*t*-Value	*P*-Value
	Mean ± SD	Mean ± SD			Mean ± SD	Mean ± SD		
FOSA- R(°)	−18.35 ± 9.23	−21.54 ± 14.26	1.562	0.021	19.27 ± 6.11	22.45 ± 5.51	2.351	0.021
FOSA- L(°)	−16.45 ± 7.86	−19.80 ± 9.81	2.203	0.029	17.02 ± 6.45	21.32 ± 7.46	2.718	0.008
O–C_2a-Np(°)	17.20 ± 8.22	13.42 ± 7.26	−2.831	0.005	19.43 ± 7.64	18.07 ± 6.94	−0.801	0.426
O–C_2a-HP(°)	11.02 ± 6.03	9.49 ± 6.08	−1.159	0.250	11.68 ± 7.11	11.59 ± 6.24	−0.039	0.969

FOSA-R: facet occiput slope angle on right side; FOSA-L: facet occiput slope angle on left side; O–C_2a-Np: O–C_2 angle in neutral position; O–C_2a-HP: O–C_2 angle in hyperflexion position.

was = 0.607. Patients with a FOSA of ≤34° were feasible for cage placement. The true AAF was neither visualized nor accessible for cage placement intraoperatively in patients with FOSA >34°.

The preoperative FOSA showed a significant positive correlation with VD ($r = 0.346$, $P = 0.008$) and a significant negative correlation with CAM ($r = -0.362$, $P = 0.005$) and age ($r = -0.265$, $P = 0.002$) (Table 5; Fig. 5A–D) and in Group A. The interobserver ICC indicated high interobserver reliability for all angles (Table 6).

Results of multiple linear regression analyses using CMA, O–C_2a-NP, O–C_2a-Hp, age, and sex as dependent variables are shown in Table 7.

4. Discussion

Proper patient positioning is crucial during posterior spine surgery, and the most commonly used position is prone. In addition to other complications related to the prone position [26–28], reaching up to the true AAF in patients with BI and AAD remains challenging for surgeons. In severe cases, reaching up to the true AAF for cage placement during surgery is impossible. We postulate that this is caused by two factors: the craniocaudal orientation of AAF in the sagittal plane, which does not change with the head's movement, and the occipital bone's position in relation to AAF that changes with the movement of the head during prone position.

We used FOSA to objectively measure the occipital bone's relationship with the AAF in the para-sagittal plane. Theoretically, in the prone position of normal people, entrance to the AAF would be impossible when the head is hyperextended as the occipital bone moves caudally and obscures the entrance to the AAF. However, in patients with BI and AAD, the C_{1}-$_{2}$ facets orient craniocaudally (posteroanterior) in the sagittal plane [9], and the atlas is located more caudally concerning the axis in the coronal view (odontoid telescoping into an atlas). Thus, even in the neutral position, the occipital bone may block entrance to the AAF in a small fraction of patients with BI and AAD.

Theoretically, reaching up to the true AAF should be impossible in all negative FOSA cases. However, this is not the case in reality for two reasons. Firstly, the surgeon does not operate precisely at 90° to the horizontal plane (FOSA is measured in the horizontal plane) but stands slightly caudally to the AAF joint level and reaches up the joint obliquely (caudocranially). Secondly, the patient's

Table 4
Patients parameters compared between pre- and postoperative periods (only patients).

Parameters	Preoperative	Postoperative	*t*-Value	*P*-Value
FOSA-R	−19.25 ± 17.32	−14.84 ± 13.87	3.417	<0.001
FOSA-L	−17.42 ± 11.14	−14.09 ± 10.54	4.051	<0.001
O–C_2a	10.38 ± 5.50	9.95 ± 6.39	0.312	0.757
CMA	131.58 ± 9.30	149.09 ± 5.15	−15.613	<0.001

FOSA-R: facet occiput slope angle on right side; FOSA-L: facet occiput slope angle on left side, CMA: cervicomedullary angle.

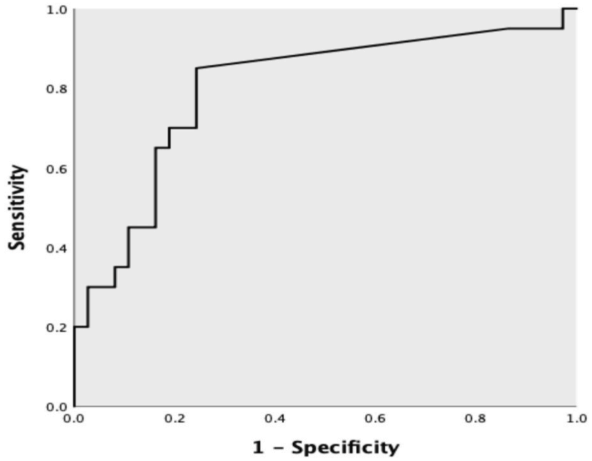

Fig. 4. Receiver operating characteristic (ROC) curve of facet-occiput slope angle (FOSA) for predicting the occurrence of cage feasibility. The area under curve (AUC) is 0.800 (95 % CI: 0.672–0.928, $P < 0.001$). The optimal cut-off point was 34°, with 85 % sensitivity and 75.7 % specificity.

Table 5
Correlation between FOSA and various parameters (only preoperative).

Parameters	FOSA	
	r-value	*P*-value
VD (mm)	0.346	0.008
ADI (mm)	0.051	0.703
O–C2a-NP(°)	−0.088	0.518
O–C2a-HP(°)	−0.105	0.492
CMA(°)	−0.362	0.005
Age (year)	−0.265	0.002
Sex	−0.17	0.047

VD: vertical distance; ADI: atlantodental interval; O–C2a-Np:O–C_2 angle in neutral position; O–C_2a-HP:O–C_2 angle in hyperflexion position; CMA: cervicomedullary angle.

upper cervical spine was positioned flexed prone "military tuck" based on the preoperative flexion O–C_2a. The inclination orientation of FOSA changes with the position of the head and, compared to the neutral position, is more positive in flexion and negative in extension positions. Therefore, negative FOSA change to positive and reaching up to the true AAF was feasible. However, in patients with a negative FOSA of mathematically greater than 34° on preoperative para-sagittal CT, reaching up to the true AAF was impossible intraoperatively even though the patient was positioned with flexed head based on the preoperative flexion O–C_2a.

Although the specificity of FOSA was poor, this value predicts the definite feasibility of cage placement intraoperatively, at least theoretically. This value was calculated using an ROC, and for angles mathematically bigger than 34°, reaching up to the true AAF was impossible intraoperatively.

During prone positioning of patients, a hyperflexed upper cervical spine will cause spinal cord compression. In contrast, overextension of the head during a prone position will cause a false larger negative FOSA. We used preoperative flexion O–C_2a as a reference, intending to decrease position-related complications in the setting of the posterior approach. Preoperative flexion radiographs are taken when the patients are awake. The patients were educated to flex their heads and reach their chin to the chest while taking radiographs. However, the patients could not flex their heads beyond the limits where protruding and unstable odontoid causes compression of the spinal cord and elicits neurological symptoms. Thus, preoperative flexion O–C_2a predicts the safe zone for every individual patient and avoids further spinal cord compression that would otherwise be caused by the overflexion of the upper cervical spine while positioning the patient for the surgery in an attempt to reach up to the true AAF.

It is vital to restore the proper occipitocervical relationship when performing occipitocervical fusion to prevent postoperative complications [29–34]. The most functional posture for the cranium on the cervical vertebra is occipitocervical "neutral" [35]. The O–C_2a is a reliable method to determine neutral occipitocervical alignment intraoperatively [30,32,34,36] with good interobserver reliability [33], correlation with surgical outcomes [29–31,35–37], and easily measured intraoperatively [31].

Both OC_2a and FOSA showed a correlation with BI. The positive O–C_2a in the neutral position decreased with the severity of BI, while negative FOSA increased. However, Pearson's correlation and linear regression did not show a significant correlation or association between the O–C_2a and FOSA. These two angles are measured in two different planes with various characteristics. The O–C_2a is not affected by the morphological variations of AAF and occiput, while FOSA is affected, which could be the possible cause of the absence of correlation between FOSA and O–C_2a. Therefore, we could not utilize preoperative flexion O–C_2a to predict the feasibility of

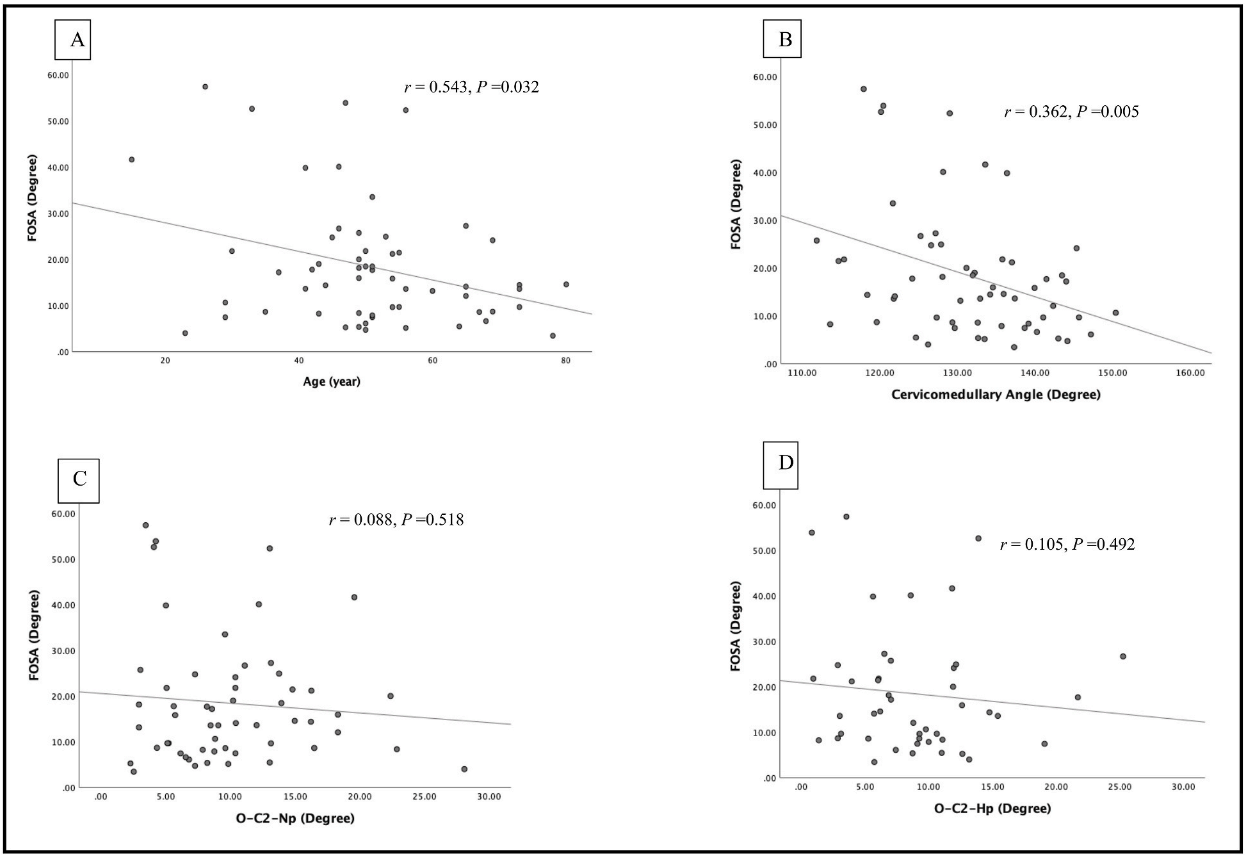

Fig. 5. **A**: Scatter diagram showing statistically significant association of age and FOSA; **B**: Scatter diagram showing statistically significant association of cervicomedullary angle and FOSA; **C**: Scatter diagram showing no statistically significant association of O–C_2a-Np angle and FOSA; **D:** Scatter diagram showing no statistically significant association of O–C_2a-Hp and FOSA.

Table 6
Interobserver interclass correlation coefficient of all parameters.

Parameters	ICC	95 % CI	*P*-Value
R-FOSA-Preop(°)	0.973	0.962–0.981	<0.001
L-FOSA-Preop(°)	0.928	0.899–0.948	<0.001
R-FOSA-Postop(°)	0.989	0.976–0.994	<0.001
L-FOSA-Postop(°)	0.977	0.953–0.989	<0.001
O–C_2a-NP-Preop(°)	0.977	0.968–0.984	<0.001
O–C_2a-NP-Postop(°)	0.978	0.956–0.989	<0.001
O–C_2a-HP-Preop(°)	0.928	0.867–0.961	<0.001

R-FOSA-Preop: preoperative facet occiput slope angle right side; L-FOSA-Preop: preoperative facet occiput slope angle left side; R-FOSA-Postop = postoperative facet-occiput slope angle right side; L-FOSA-Postop: postoperative facet-occiput-slope angle left side; O–C_2a-Np: O–C_2 angle in neutral position; O–C_2a-HP: O–C_2 angle in hyperflexion position; Preop: preoperative; Postop: postoperative; ICC: interclass coefficient.

cage placement directly.

AAD is associated with variable patient age at presentation [2]. FOSA showed a significant negative association with age and CMA in our patients. Younger patients with smaller CMA showed larger FOSA.

The more oblique the inferior facet of the atlas, the larger the negative FOSA; the right inferior articular facet of the atlas was more oblique than the left one, according to a morphometric analysis of the atlantoaxial assimilated vertebral specimen [38]. Therefore, the mean value of negative FOSA was larger on the right side than on the left.

Postoperative FOSA was significantly smaller than preoperative, and on both sides, the two sides of AAF were levered and brought to horizontal balance in the coronal plane after the surgery. The mean value of FOSA was significantly larger in females than in males in both groups ($P < 0.05$), and the number of female patients was significantly higher than the males.

The limitations of this study are: 1. We only studied patients of our hospital (single-centered), 2. Patients' number is not high, 3. The

Table 7
Association of age or CMA with FOSA from the multiple regression analysis (only preoperative).

	B	95 % Confidence interval		β	P
		Lower limit	Upper limit		
CMA(°)	−0.518	−0.875	−0.161	−0.362	0.005
O–C_2a-Np (°)	−0.199	−0.893	0.496	−0.084	0.566
O–C2a-Hp (°)	−0.054	−0.825	0.717	−0.021	0.887
Age (year)	−0.315	−0.600	−0.029	−0.324	0.032
Sex	−6.113	−14.265	2.039	−0.217	0.137

all coefficients were adjusted for age, and sex; R^2: 0.237; B, unstandardized regression coefficient; β, standardized regression coefficient; OC_2a-Np: O–C_2 angle in neutral position; OC_2a-Hp:O–C_2 angle in hyperflexion position; CMA: cervicomedullary angle.

three-dimensional cage cannot used in severe osteoporotic patients and children with immature bone growth, 4. Short follow-up time. A larger multi-institutional study should be conducted to predict the feasibility of placement based on preoperative FOSA more accurately.

5. Conclusion

Direct posterior reduction and manipulation of the C_{1-2} joints accompanied by placement of spacers is the state-of-the-art technique for treating BI and AAD. The hindrance of occiput to reaching up to the true AAF during operation is crucial for cage placement. FOSA can objectively measure the feasibility of intraoperative cage placement when the patient is positioned prone per preoperative flexion O–C_2a. A FOSA $>34^o$ is contraindication for cage placement.

Funding

Initiation of Key Research Projects in Higher Education Institutions in Henan Province; 3D-printing anatomical-oriented universal lateral mass fusion cage application research (Fund number: 225320076)

Data availability statement

The data associated with this study has not been deposited into a publicly available repository.
The data will be made available on request.

CRediT authorship contribution statement

Mirwais Alizada: Conceptualization, Writing – review & editing, Methodology, Software, Writing – original draft. **Yuqiang Wang:** Data curation, Formal analysis, Software. **Yao Zhao:** Formal analysis, Writing – original draft. **Shuhao Zhang:** Formal analysis, Writing – original draft. **Gati Hayatullah:** Data curation, Formal analysis, Software. **Min Zhang:** Software, Writing – original draft. **Shuxin Li:** Data curation, Formal analysis. **Kejdi Lalaj:** Software, Writing – original draft. **Kerong Yang:** Data curation, Formal analysis, Writing – original draft. **Ismatullah Soufiany:** Data curation, Formal analysis, Writing – original draft. **Limin Wang:** Conceptualization, Methodology, Supervision. **Yilin Liu:** Conceptualization, Funding acquisition, Methodology.

Declaration of competing interest

The authors declare that they have no known competing financial interests or personal relationships that could have appeared to influence the work reported in this paper.

Abbreviations

3D	Three dimensional
AAD	Atlantoaxial dislocation
AAF	Atlantoaxial facets
ADI	Atlantodental interval
AUC	Area under the curve
BI	Basilar Invagination
CMA	Cervicomedullary angle
CSF	Cerebrospinal fluid
CT	Computed tomography
CVJ	Craniocervical junction
FOSA	Facet-occiput slope angle

ICC	Intraclass correlation coefficient
ICU	Intensive care unit
MRA	Magnetic resonance angiography
MRI	Magnetic resonance image
O–C_2a	Occipital C_2 angle
ROC	Receiver operative curve
SI	Sagittal inclination
VD	Vertical distance

References

[1] P. Salunke, M. Karthigeyan, N. Sunil, V. Rangan, "Congenital anomalies of craniovertebral junction presenting after 50 years of age": an oxymoron or an unusual variation? Clin. Neurol. Neurosurg. 165 (2018) 15–20, https://doi.org/10.1016/J.CLINEURO.2017.12.015.

[2] P. Salunke, M. Sharma, Congenital atlantoaxial dislocation: a dynamic process and role of facets in irreducibility, Journal of Neurosurgery: Spine 15, no.6 (2011) 678-685, https://thejns.org/spine/view/journals/j-neurosurg-spine/15/6/article-p678.xml.

[3] A. Goel, Treatment of basilar invagination by atlantoaxial joint distraction and direct lateral mass fixation, J. Neurosurg. Spine 1 (2004) 281–286, https://doi.org/10.3171/SPI.2004.1.3.0281.

[4] F. Jian, Z. Chen, K. Wrede, M. Samii, F.L. Neurosurgery, undefined, Direct Posterior Reduction and Fixation for the Treatment of Basilar Invagination with Atlantoaxial Dislocation, Academic.Oup.Com, 2010 (n.d.), https://academic.oup.com/neurosurgery/article-abstract/66/4/678/2680752. (Accessed 22 December 2021).

[5] P.S. Chandra, A. Kumar, A. Chauhan, A. Ansari, N.K. Mishra, B.S. Sharma, Distraction, compression, and extension reduction of basilar invagination and atlantoaxial dislocation: a novel pilot technique, Neurosurgery 72 (2013) 1040–1053, https://doi.org/10.1227/NEU.0b013e31828bf342.

[6] B. Suh, M. Padua, K. Riew, A New Technique for Reduction of Atlantoaxial Subluxation Using a Simple Tool during Posterior Segmental Screw Fixation, H.K.-… of N. Spine, undefined, Thejns.Org. (n.d., 2013, https://thejns.org/spine/view/journals/j-neurosurg-spine/19/2/article-p160.xml. (Accessed 6 January 2023).

[7] Y. Yin, G. Qiao, X. Yu, H. Tong, Y.Z.-T.S. Journal, undefined, Posterior Realignment of Irreducible Atlantoaxial Dislocation with C1–C2 Screw and Rod System: a Technique of Direct Reduction and Fixation, Elsevier, 2013 (n.d.), https://www.sciencedirect.com/science/article/pii/S1529943013014617. (Accessed 6 January 2023).

[8] A. Goel, A. Kulkarni, Reduction of Fixed Atlantoaxial Dislocation in 24 Cases, P.S.-J. of N. Spine, undefined, Thejns.Org., 2005, https://thejns.org/spine/view/journals/j-neurosurg-spine/2/4/article-p505.xml. (Accessed 6 January 2023).

[9] A. Goel, A. Shah, S. Rajan, Vertical mobile and reducible atlantoaxial dislocation: clinical article, J. Neurosurg. Spine 11 (2009) 9–14, https://doi.org/10.3171/2009.3.SPINE08927.

[10] P. Chandra, M. Prabhu, N. Goyal, Distraction, Compression, Extension, and Reduction Combined with Joint Remodeling and Extra-articular Distraction: Description of 2 New Modifications for its Application, A.G.-, undefined, Academic.Oup.Com, 2015, https://academic.oup.com/neurosurgery/article-abstract/77/1/67/2452086.

[11] P. Salunke, S. Futane, M. Sharma, S. Sahoo, U. kovilapu, N.K. Khandelwal, "Pseudofacets" or "supernumerary facets" in congenital atlanto-axial dislocation: boon or bane? Eur. Spine J. 24 (2015) 80–87, https://doi.org/10.1007/S00586-014-3485-6.

[12] Y.H. Yin, X.G. Yu, D.B. Zhou, P. Wang, Y.Z. Zhang, X.D. Ma, B. Bu, Three-dimensional Configuration and Morphometric Analysis of the Lateral Atlantoaxial Articulation in Congenital Anomaly with Occipitalization of the Atlas, Spine (Phila Pa 1976), 2012, p. 37, https://doi.org/10.1097/BRS.0B013E318227EFE7.

[13] P. Sarat Chandra, J. Bajaj, P.K. Singh, K. Garg, D. Agarwal, Basilar invagination and atlantoaxial dislocation: reduction, deformity correction and realignment using the DCER (distraction, compression, extension, and reduction) technique with customized instrumentation and implants, Neurospine 16 (2019) 231–250, https://doi.org/10.14245/ns.1938194.097.

[14] J. Yeom, D. Kafle, N. Nguyen, W. Noh, K.P.-T.S. Journal, undefined, Routine Insertion of the Lateral Mass Screw via the Posterior Arch for C1 Fixation: Feasibility and Related Complications, Elsevier, 2012 (n.d. https://www.sciencedirect.com/science/article/pii/S1529943012004342. (Accessed 22 January 2023).

[15] M. Tan, H. Wang, Y. Wang, G. Zhang, P. Yi, Z. Li, Morphometric Evaluation of Screw Fixation in Atlas via Posterior Arch and Lateral Mass, H.W.- Spine, undefined, Journals.Lww.Com., 2003, https://journals.lww.com/spinejournal/Fulltext/2003/05010/Anatomic_Consideration_of_C2_Pedicle_Screw.00010.aspx. (Accessed 22 January 2023).

[16] N.W.-C.S. Surgery, undefined, Posterior C2 Fixation Using Bilateral, Crossing C2 Laminar Screws: Case Series and Technical Note, Journals.Lww.Com., 2004 n.d.), https://journals.lww.com/jspinaldisorders/Fulltext/2004/04000/Posterior_C2_Fixation_Using_Bilateral. (Accessed 22 January 2023).

[17] J. Harms, R.M. Spine, undefined, Posterior C1–C2 fusion with polyaxial screw and rod fixation, Journals.Lww.Com. 26 (2001). https://journals.lww.com/spinejournal/fulltext/2001/11150/posterior_c1_c2_fusion_with_polyaxial_screw_and.14.aspx. (Accessed 22 January 2023).

[18] Quantitative Anatomic Study of Atlando-Odontoid Joint and Design of an Artificial , (n.d.)..

[19] X. Huang, Q. Yin, Z. Wang, H. Xia, Implantation of the anterior atlantoaxial lateral mass intervertebral cage using the transoral approach, J. Orthop. Sci. 22 (2017) 630–634, https://doi.org/10.1016/j.jos.2017.02.011.

[20] W.R.K. Smoker, G. Khanna, Imaging the craniocervical junction, Child's Nerv. Syst. 24 (2008) 1123–1145, https://doi.org/10.1007/S00381-008-0601-0.

[21] T. Inoue, K. Ito, · Kei Ando, Kazuyoshi Kobayashi, H. Nakashima, Y. Katayama, Masaaki Machino, S. Kanbara, S. Ito, H. Yamaguchi, H. Koshimizu, F. Kato, Shiro Imagama, Age-related changes in upper and lower cervical alignment and range of motion: normative data of 600 asymptomatic individuals, Eur. Spine J.. 29 (1234) 2378–2383. https://doi.org/10.1007/s00586-020-06547-9..

[22] P. Salunke, S.K. Sahoo, A.N. Deepak, N.K. Khandelwal, Redefining congenital atlantoaxial dislocation: objective assessment in each plane before and after operation, World Neurosurg 95 (2016) 156–164, https://doi.org/10.1016/j.wneu.2016.07.097.

[23] J.E. Fischer, L.M. Bachmann, R. Jaeschke, A readers' guide to the interpretation of diagnostic test properties: clinical example of sepsis, Intensive Care Med. 29 (2003) 1043–1051, https://doi.org/10.1007/S00134-003-1761-8.

[24] R. Fluss, D. Faraggi, B. Reiser, Estimation of the Youden Index and its associated cutoff point, Biom. J. 47 (2005) 458–472, https://doi.org/10.1002/BIMJ.200410135.

[25] N.J. Perkins, E.F. Schisterman, A. Vexler, Original Contribution Receiver Operating Characteristic Curve Inference from a Sample with a Limit of Detection, (n.d.). https://doi.org/10.1093/aje/kwk011..

[26] J.A.-B.J. of Anaesthesia, undefined, The Prone Position for the Surgical Patient: a Historical Review of the Principles and Hazards, 1991. Citeseer. (n.d.), https://citeseerx.ist.psu.edu/document?repid=rep1&type=pdf&doi=c80009cd34857eac246bd65ae20bbab4625137ee. (Accessed 7 January 2023).

[27] M. Kwee, Y. Ho, W.R.-I. surgery, undefined, The Prone Position during Surgery and its Complications: a Systematic Review and Evidence-Based Guidelines, Allenpress.Com., Meridian, 2015. https://meridian.allenpress.com/international-surgery/article-abstract/100/2/292/175367. (Accessed 7 January 2023).

[28] I. Kamel, R. Barnette, Positioning patients for spine surgery: avoiding uncommon position-related complications, World J. Orthoped. 5 (2014) 425–443, https://doi.org/10.5312/WJO.V5.I4.425.

[29] V. Sheshadri, R. Moga, P. Manninen, C.L. Goldstein, Y.R. Rampersaud, E.M. Massicotte, M.G. Fehlings, L. Venkatraghavan, Airway adverse events following posterior occipito-cervical spinal fusion, J. Clin. Neurosci. 39 (2017) 124–129, https://doi.org/10.1016/J.JOCN.2016.12.036.

[30] M. Izeki, M. Neo, H. Ito, K. Nagai, T. Ishizaki, T.O. Spine, Reduction of Atlantoaxial Subluxation Causes Airway Stenosis, undefined, Journals.Lww.Com., 2013. n.d.), https://journals.lww.com/spinejournal/Fulltext/2013/04200/Reduction_of_Atlantoaxial_Subluxation_Causes.15.aspx. (Accessed 7 January 2023).

[31] M. Miyata, M. Neo, S. Fujibayashi, H. Ito, M. Takemoto, T. Nakamura, O-C2 Angle as a Predictor of Dyspnea And/or Dysphagia after Occipitocervical Fusion, vol. 34, Spine (Phila Pa 1976), 2009, pp. 184–188, https://doi.org/10.1097/BRS.0B013E31818FF64E.

[32] T. Takami, T. Ichinose, K. Ishibashi, T. Goto, N. Tsuyuguchi, K. Ohata, Importance of fixation angle in posterior instrumented occipitocervical fusion—technical note, Jstage.Jst.Go.Jp. 48 (2008). https://www.jstage.jst.go.jp/article/nmc/48/6/48_6_279/_article/-char/ja/. (Accessed 7 January 2023).

[33] S. Iyer, L. Lenke, V. Nemani, M. Fu, Variations in Occipitocervical and Cervicothoracic Alignment Parameters Based on Age: a Prospective Study of Asymptomatic Volunteers Using Full-Body Radiographs, G.S.- Spine, undefined, Journals.Lww.Com, 2016 (n.d.), https://journals.lww.com/spinejournal/Fulltext/2016/12010/Variations_in_Occipitocervical_and_Cervicothoracic.12.aspx. (Accessed 7 January 2023).

[34] N. Shoda, K. Takeshita, A. Seichi, T. Akune, Measurement of Occipitocervical Angle, S.N.- Spine, undefined, Journals.Lww.Com, 2004 (n.d.), https://journals.lww.com/spinejournal/fulltext/2004/05150/measurement_of_occipitocervical_angle.22.aspx. (Accessed 7 January 2023).

[35] F.M. Phillips, C.S. Phillips, F.T. Wetzel, C. Gelinas, Occipitocervical Neutral Position: Possible Surgical Implications, Spine (Phila Pa 1976), 1999, p. 24, https://doi.org/10.1097/00007632-199904150-00008.

[36] M. Izeki, M. Neo, M. Takemoto, S. Fujibayashi, H. Ito, K. Nagai, S. Matsuda, The O-C2 angle established at occipito-cervical fusion dictates the patient's destiny in terms of postoperative dyspnea and/or dysphagia, Eur. Spine J. 23 (2014) 328–336, https://doi.org/10.1007/S00586-013-2963-6.

[37] Y. Meng, T. Wu, Z. Liu, D. Wen, X. Rong, H. Chen, J. Lou, H. Liu, The impact of the difference in O-C2 angle in the development of dysphagia after occipitocervical fusion: a simulation study in normal volunteers combined with a case-control study, Spine J. 18 (2018) 1388–1397, https://doi.org/10.1016/J.SPINEE.2018.01.005.

[38] A.M. Ryniewicz, J. Skrzat, J.A. Walocha, Geometry of the Articular Facets of the Lateral Atlanto-Axial Joints in the Case of Occipitalization Heart Ablation View Project 3D Printed Anatomical Models View Project, 2010. https://www.researchgate.net/publication/49679860.